

GTP Binding Induces Filament Assembly of a Recombinant Septin

Manuel Mendoza,^{1,4} Anthony A. Hyman,²
and Michael Glotzer^{1,3}

¹Research Institute of Molecular Pathology
Dr. Bohr-Gasse 7
A-1030 Vienna
Austria

²Max Planck Institute of Molecular Cell Biology
and Genetics
Pflanzstrasse 108
01307 Dresden
Germany

Summary

The septins are a family of GTPases involved in cytokinesis in budding yeast, *Drosophila*, and vertebrates (see [1] for review). Septins are associated with a system of 10 nm filaments at the *S. cerevisiae* bud neck, and heteromultimeric septin complexes have been isolated from cell extracts in a filamentous state [2–4]. A number of septins have been shown to bind and hydrolyze guanine nucleotide [2, 5, 6]. However, the role of GTP binding and hydrolysis in filament formation has not been elucidated. Furthermore, several lines of evidence suggest that not all the subunits of the septin complex are required for all aspects of septin function [3, 7]. To address these questions, we have reconstituted filament assembly in vitro by using a recombinant *Xenopus* septin, *XI* Sept2. Filament assembly is GTP dependent; moreover, the coiled-coil domain common to most septins is not essential for filament formation. Septin polymerization is preceded by a lag phase, suggesting a cooperative assembly mechanism. The slowly hydrolyzable GTP analog, GTP- γ -S, also induces polymerization, indicating that polymerization does not require GTP hydrolysis. If the properties of *XI* Sept2 filaments reflect those of native septin complexes, these results imply that the growth or stability of septin filaments, or both, is regulated by the state of bound nucleotide.

Results and Discussion

To obtain large amounts of septin protein, a *Xenopus* septin, *XI* Sept2, was expressed in *E. coli*, and the protein was purified by affinity column chromatography. The purity of the column eluate exceeded 90%, as judged by Coomassie-stained acrylamide gels (Figure 1A). Furthermore, the preparation ran as a single peak of apparent molecular weight of 87 kDa on a gel filtration column, compatible with it being a monomer or a very stable dimer (Figure 1B). Like all known septins, *XI* Sept2 contains a P loop motif and other sequences characteristic of GTP binding proteins [8]. The human gene most re-

lated to *XI* Sept2 is now known as Sept2 (BAA05893) [9]; that of budding yeast is Cdc3p. No protein bound nucleotide was detected in our septin preparations (as assessed by HPLC over a MonoQ column; our unpublished data). We therefore tested the ability of recombinant *XI* Sept2 to bind and hydrolyze exogenous guanine nucleotide. Using a filter binding assay, we found that *XI* Sept2 bound to radiolabeled GTP, whereas the BSA control showed no detectable binding (Figure 1C). Based on these experiments, we estimate that 40%–50% of the septin in our preparation is competent for GTP binding. Binding is specific for GTP; unlabeled GTP, but not ATP or GDP, efficiently compete with the radiolabeled guanine nucleotide. Unlabeled GTP- γ -S competed for binding as efficiently as GTP (Figure 1E). The rate of GTP binding is slower than would be expected for binding of a small molecule. This may indicate that a conformational change is required for the protein to bind nucleotide; it is also possible that although the recombinant protein is soluble, it is not perfectly folded and the slow binding is due to partial refolding. To assess nucleotide hydrolysis, we incubated *XI* Sept2 with [α -³²P]GTP or GTP- γ -[³⁵S], and the production of radioactive GDP or free thio-phosphate was followed by thin layer chromatography (TLC). GTP, but not GTP- γ -S, was efficiently hydrolyzed (Figure 1D). On the other hand, addition of 10 units of alkaline phosphatase to the GTP- γ -S-containing sample resulted in >70% hydrolysis within 60 min (our unpublished data). Thus, *XI* Sept2 readily binds and hydrolyzes exogenous GTP.

Filament-forming proteins such as actin, tubulin, and FtsZ polymerize in a nucleotide-dependent manner. To determine whether *XI* Sept2 can assemble into filaments in the presence of guanine nucleotide, we incubated the protein with GTP or GTP- γ -S and subsequently adsorbed it to glass coverslips. The coverslips were then fixed and stained with anti-*XI* Sept2 antibody. Under these conditions, immunofluorescence microscopy revealed filamentous structures of up to 7 μ m in length (Figure 2A). These filaments were of uniform intensity along their lengths, suggesting a constant width. Filaments were not observed when *XI* Sept2 was incubated with ATP or GDP (Figure 2A). The structure of *XI* Sept2 filaments was examined by transmission electron microscopy (Figure 2B). Short filaments (with a length between 200 and 1000 nm) could be detected in reactions that had been incubated with GTP for 5 min, whereas longer incubation periods resulted in filaments \geq 1000 nm long (Figure 2B, upper left panel). The width of the filaments was estimated to be approximately 20 nm. In the absence of added nucleotide or in the presence of ATP, small amorphous aggregates were observed, confirming that filament formation requires GTP (Figure 2B, upper right). At high magnification, a narrow region of electron-dense material was visible along the filament lengths (Figure 2B, lower left), suggesting that the 20 nm-wide structures are composed of two 8–9 nm-wide filaments in close apposition. This can be compared with the reported width (7–9 nm) of septin filaments

³Correspondence: mglotzer@nt.imp.univie.ac.at

⁴Present address: European Molecular Biology Laboratory, Meyerhofstr. 1, 69117 Heidelberg, Germany.

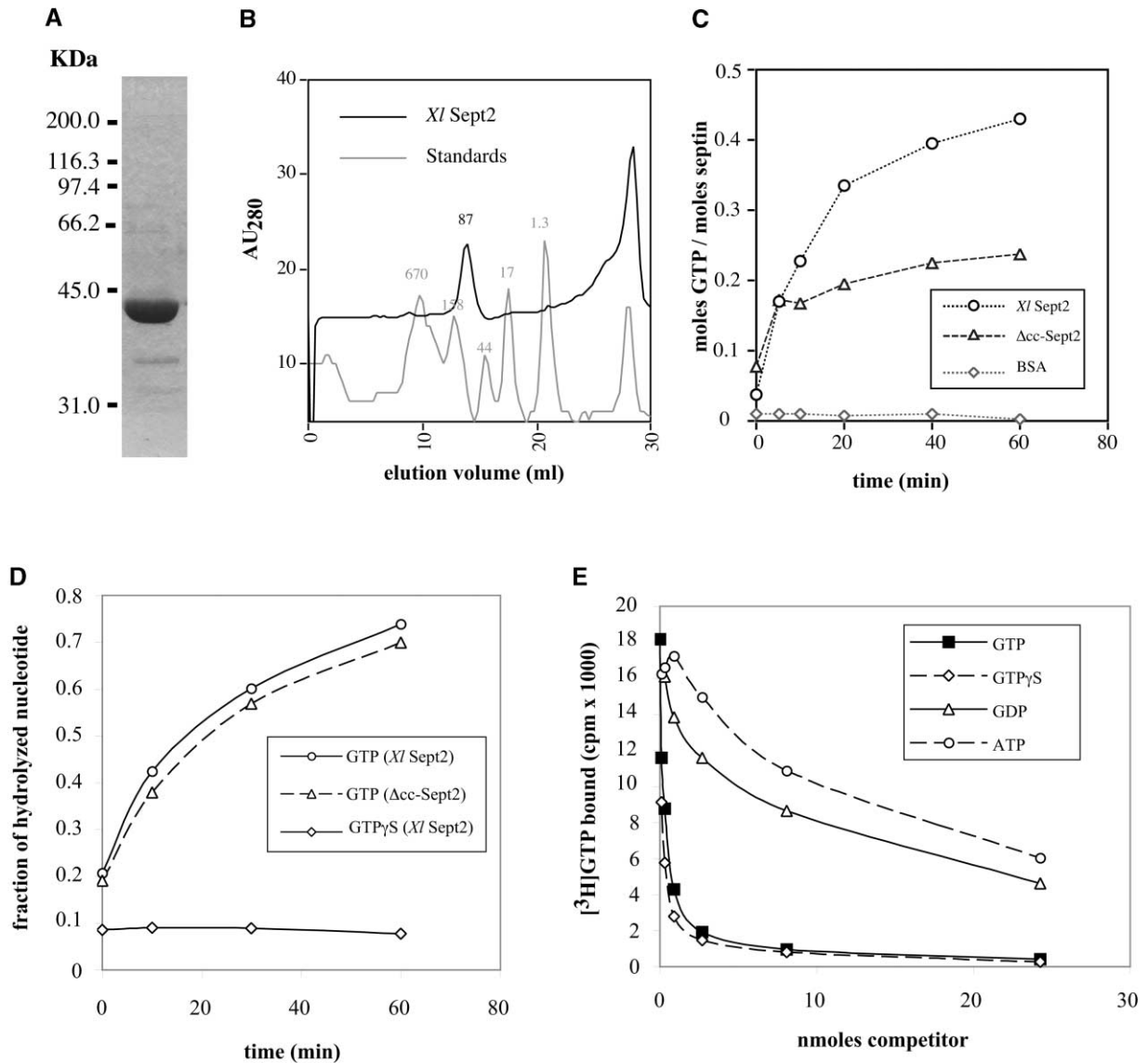


Figure 1. *XI* Sept2 Binds and Hydrolyzes GTP

(A) A Coomassie-stained acrylamide gel showing affinity-purified *XI* Sept2. The major band corresponds to the expected *XI* Sept2 molecular weight of 41 kDa.

(B) Gel filtration of purified *XI* Sept2 and a set of molecular weight standards (Pharmacia) on a Superdex 200 column.

(C) [³H]GTP binding of *XI* Sept2 and Δ cc-Sept2, as determined by a filter binding assay. A total of 1 μ M septin was incubated with 4.4 μ M GTP and 5 mM MgCl₂.

(D) Nucleotide hydrolysis by *XI* Sept2 and Δ cc-Sept2, as assayed by TLC. BSA was used as a negative control in both experiments.

(E) Competition of GTP binding. A total of 200 pmoles *XI* Sept2 (1 μ M) was incubated with 4.4 μ M [³H]GTP and the indicated amounts of nonlabeled GTP, GTP- γ -S, GDP, or ATP.

purified from *Drosophila* and yeast cell extracts [2, 3]. Moreover, structures reminiscent of the paired filaments described here have been observed when the purified yeast septin complex is dialyzed into a low-salt buffer; in this case, filaments within a doublet were spaced by a variable (2–20 nm) gap without sign of a bridging structure [3]. A minority of *XI* Sept2 filaments associated laterally to form small bundles (Figure 2B). The presence of guanine nucleotide is therefore sufficient to induce assembly of a single septin into filamentous structures.

Many (but not all) of the known septins contain C-ter-

минаl sequences predicted to form a coiled-coil. However, the importance of these domains in septin function(s) has not been addressed previously. We have generated a septin protein lacking the coiled-coil domain (Δ cc-Sept2) and have characterized its GTPase- and filament-formation activities. Δ cc-Sept2 maintained GTPase activity, albeit with a reduced GTP binding efficiency (Figures 1C and 1D). This could indicate that a larger fraction of the truncated protein fails to fold correctly in the bacterial cell as compared to the full-length septin. Importantly, purified Δ cc-Sept2 was able

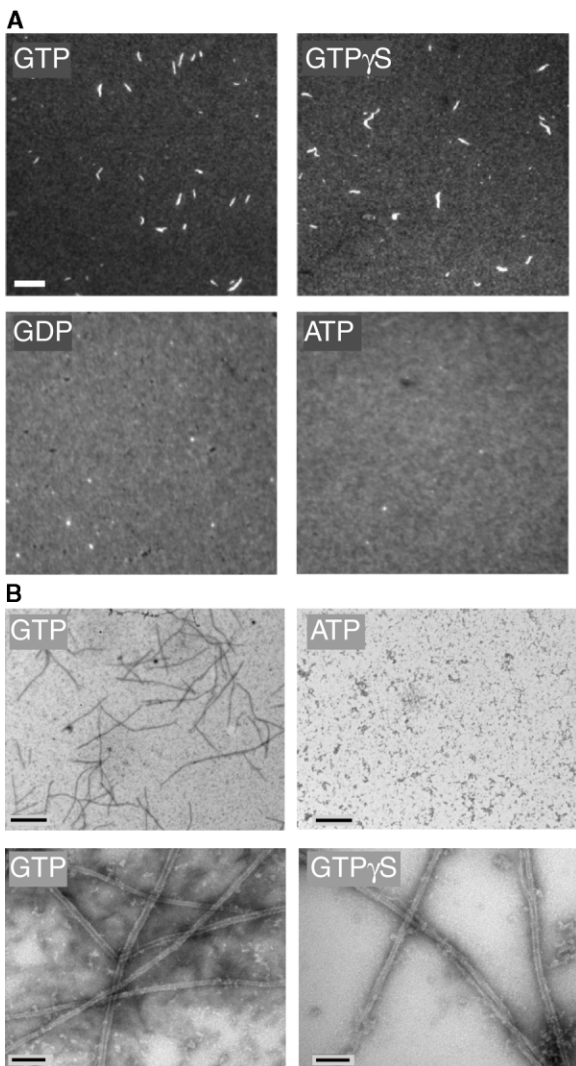


Figure 2. GTP-Dependent Assembly of *XI* Sept2

(A) Immunostainings of septin preparations (25 μ M) incubated with the indicated nucleotide for 30 min. Filamentous structures are observed only in the presence of GTP or GTP- γ -S. The scale bar represents 2 μ m.

(B) Electron microscopy of *XI* Sept2 filaments. Upper panels: a low-magnification image showing 20 nm wide septin filaments in the presence of GTP; no filaments are observed in the presence of ATP (the scale bar represents 2 μ m). Lower panels: high-magnification images of GTP- or GTP- γ -S-containing reactions, where the 20 nm wide filaments appear to be composed of two thinner (8–9 nm) filaments in close association (the scale bar represents 100 nm).

to assemble into filaments in the presence of GTP, as judged by immunofluorescence and EM (Figure 3). Moreover, coassembly between full-length *XI* Sept2 and a biotinylated form of Δ cc-Sept2 was also observed by immunofluorescence, for which anti-*XI* Sept2 antibody was used in conjunction with fluorophore-coupled streptavidin (our unpublished data). When polymerized under equivalent conditions, Δ cc-Sept2 filaments were less abundant than *XI* Sept2 filaments (compare GTP panels in Figures 2A and 3A). Thus, the filament formation ability of *XI* Sept2 is diminished, but not abolished, by deletion of the coiled-coil domain.

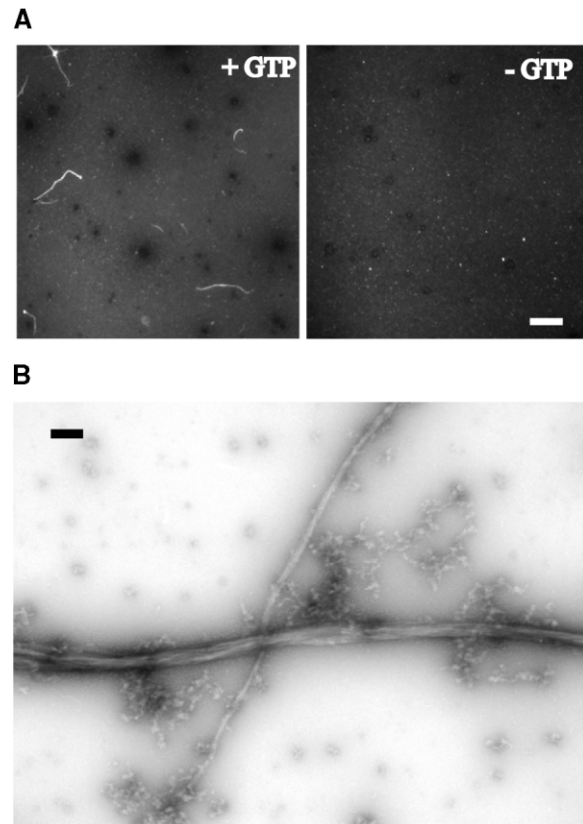


Figure 3. Filament Assembly Does Not Require the Coiled-Coil Domain

(A) Immunofluorescence images of Δ cc-*XI* Sept2 filaments prepared as in Figure 2A. The scale bar represents 1.2 μ m.

(B) An electron micrograph of Δ cc-*XI* Sept2 filament bundles. The scale bar represents 200 nm.

In order to gain insights into the septin polymerization mechanism, we examined the kinetics of *XI* Sept2 filament assembly by right-angle light scattering. This method has been used for studying the polymerization of filament-forming proteins such as actin and FtsZ. It has been shown that the intensity of scattered light is linear relative to polymer mass and that this relationship is largely independent of filament length [10–12]. Scattered-light measurements are sensitive to changes in filament width that could be caused by filament bundling (e.g., [13]; however, light and electron microscopy of septin filaments indicate that only a minor fraction of septin filaments are bundled [see Figure 2]). When GDP or ATP was added to *XI* Sept2, the level of scattered light remained stable for the entire duration of the experiment over a wide range of *XI* Sept2 concentrations (1–20 μ M). The addition of GTP resulted in a rapid increase in light scattering after a lag phase; filament assembly was then followed by a steady-state phase in which polymer content remained constant over time (Figure 4A). The duration of the lag phase was inversely proportional to *XI* Sept2 concentration. The lag phase is not solely due to the slow kinetics of nucleotide binding, which is independent of *XI* Sept2 concentration (our unpublished data). A lag phase is suggestive of a nucleated polymer-

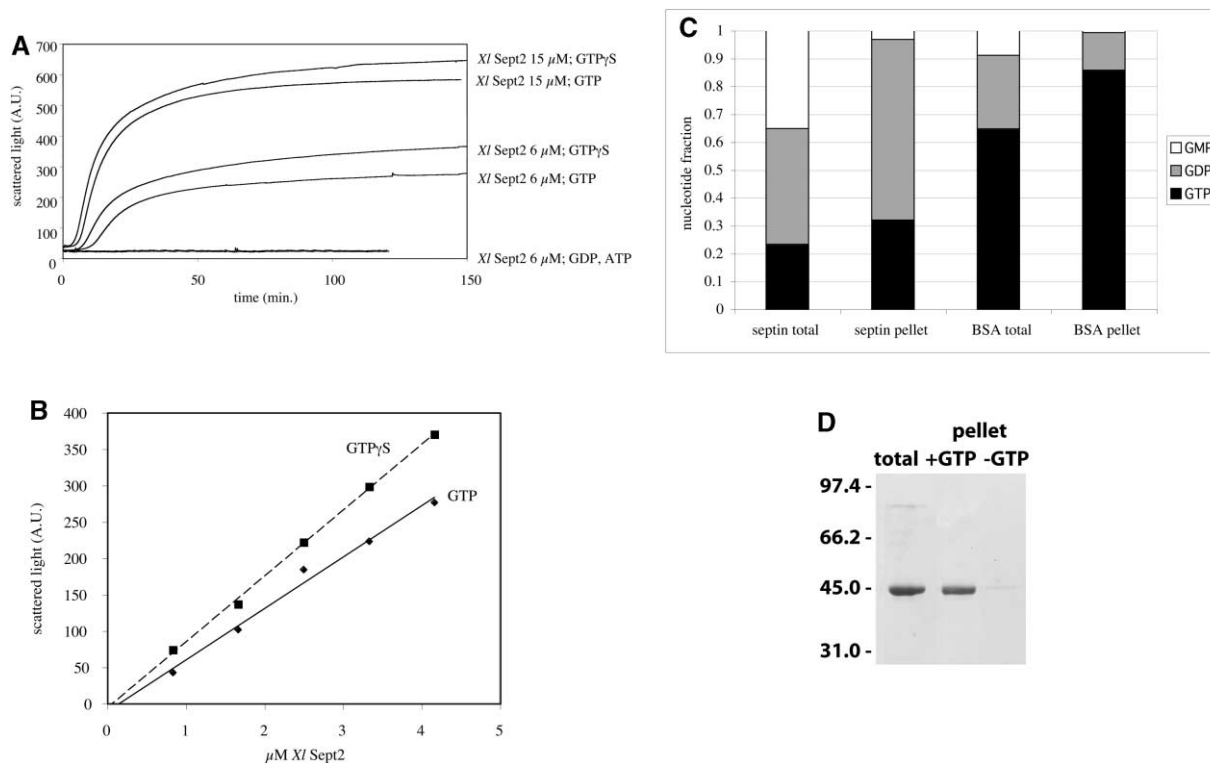


Figure 4. Quantification of *XI Sept2* Filament Assembly by Right Angle Light Scattering

- (A) Time courses of filament assembly in the presence of 0.5 mM GTP and GTP- γ -S at different *XI Sept2* concentrations. After nucleotide addition, the cuvette was repositioned in the spectrometer at time = 0 min.
- (B) Estimation of the critical concentration for filament assembly in the presence of 0.5 mM GTP and GTP- γ -S.
- (C) Analysis of nucleotide bound to septin filaments. Septin polymer was isolated by sedimentation, and the nucleotide present in the total reaction and that bound to polymer were extracted and analyzed by TLC. Since the pellets were too fragile to wash, some nucleotide was recovered in the negative control; however, significantly more nucleotide pelleted in the presence of *XI Sept2* polymer.
- (D) A Coomassie gel of the sedimentation reaction demonstrating that sedimentation of septin is GTP dependent.

ization mechanism, in which initiation of filament assembly is the rate-limiting process and is followed by a relatively faster elongation of polymer nuclei [14].

We sought to examine the role of GTP hydrolysis in the polymerization kinetics of *XI Sept2*. To this aim, we used the GTP analog GTP- γ -S, which binds to *XI Sept2* with the same affinity as GTP but fails to be hydrolyzed (see Figures 1D and 1E). The use of GTP- γ -S in polymerization reactions did not significantly alter the length of the lag phase (compare plots in Figure 4A). However, equal concentrations of *XI Sept2* yielded a higher degree of polymerization at steady state in the presence of GTP- γ -S than in the presence of GTP. Hence, the equilibrium between monomeric and polymeric septin appears to be shifted toward polymer formation when nucleotide hydrolysis is inhibited. Although filament bundling could also account for this relative increase, EM analysis did not indicate a significant increase in bundling in the presence of GTP- γ -S (Figure 2). Several alternative mechanisms could account for the differences seen between GTP- and GTP- γ -S-induced polymerization. Septin filaments bound to GDP could be less stable than filaments bound to GTP (or GTP- γ -S). Additionally, monomeric GDP bound *XI Sept2* may accumulate in the reaction and have a lower affinity for filament ends than GTP bound monomer. Indeed, we have found that under

the conditions used to measure polymerization in Figure 4A, up to 70% of *XI Sept2* is bound to GDP 60 min after nucleotide addition (see Experimental Procedures). Therefore, our data are compatible with either of these two mechanisms (or both) accounting for the different polymerization capabilities of *XI Sept2* in the presence of GTP and GTP- γ -S. Importantly, these data confirm that filament assembly does not require GTP hydrolysis.

Although *XI Sept2* can polymerize in the presence of GTP- γ -S, which is not hydrolyzed to a detectable extent, the data in Figure 1 indicate that *XI Sept2* does hydrolyze GTP. Therefore, we determined the state of the nucleotide bound to polymeric *XI Sept2*. Septin filaments that were assembled in the presence of ^{32}P - α -GTP (25 μM Sept2, 500 μM GTP) were sedimented through a glycerol cushion to isolate polymeric *XI Sept2*. SDS-PAGE analysis showed that under these conditions septin protein sediments in a GTP-dependent manner (Figure 4D). The nucleotide bound to polymeric septin was extracted and resolved by TLC. We found that the GDP:GTP ratio was 2:1 both in the unfractionated septin reaction and in the fraction containing polymeric septin (Figure 4C). Although significant amounts (30%) of GMP were also present in the unfractionated reaction, no GMP was present in the pellet. Thus, both GDP and GTP are present in polymeric septin. These data further confirm that

polymerization is not directly coupled to nucleotide hydrolysis, which is consistent with the observation that GTP- γ -S also supports polymerization.

If *Xl Sept2* forms nucleated polymers, there ought to be a “critical concentration” for filament assembly. This is defined as the concentration below which nucleation cannot occur and only monomers (and a small number of short oligomers) exist. Above the critical concentration, nucleated polymers assemble and are in equilibrium with the monomeric form. The most reliable method of measuring the critical concentration is to dilute preassembled polymer to a variety of concentrations and to determine the concentration below which all filaments disassemble. This experimental procedure is preferred over initiating assembly at different concentrations because near the critical concentration, the long lag phases and low elongation rates make it difficult to assess when steady state has been reached. We therefore assembled *Xl Sept2* filaments to steady state in the presence of either GTP or GTP- γ -S, diluted them to different protein concentrations, and let them equilibrate to a new steady state. Measurements of the polymer content by light scattering showed that filaments were still present at all the concentrations tested (0.8–4.2 μ M). The data points fitted a linear plot that, when extrapolated to zero polymer content, predicts a critical concentration of 0.2 μ M and 0.07 μ M in the presence of GTP and GTP- γ -S, respectively, although these are rough estimates (Figure 4B). Because of the low signal-to-noise ratio at lower protein concentrations, we were unable to directly measure the critical concentration with this assay. However, we have followed depolymerization by indirect immunofluorescence of *Xl Sept2* filaments and have established that septin filaments assembled in the presence of GTP or GTP- γ -S and diluted below 0.05 μ M disassemble; in the case of GTP-assembled filaments, filaments are no longer detectable after a few minutes at room temperature, suggesting that the critical concentration is different from zero (our unpublished data).

Conclusions

In this paper, we have shown that a single vertebrate septin assembles into filaments upon addition of GTP. This finding has been documented by immunofluorescence, electron microscopy, and light-scattering measurements. Filament assembly does not require GTP hydrolysis; indeed, the extent of filament assembly is greater in the presence of GTP- γ -S. In addition, we show that filament assembly is stimulated by, but not wholly dependent on, the coiled-coil domain that is found in most, but not all, septin proteins. Finally, kinetic analysis of polymerization suggests that septin filaments assemble as a nucleated polymer.

Biochemical studies have established that septins exist in heteromultimeric complexes [2–4]. In budding yeast, however, the *CDC10* septin can be deleted without compromising cell viability [3]. Furthermore, in *Drosophila*, though two additional septins copurify with the Pnut septin, recent evidence indicates that Sep2, but not Sep1, still localizes to the leading edge of cleavage furrows in the absence of Pnut [7]. Therefore, not all

the subunits in the septin complex are required for all aspects of septin function in these organisms. In this paper, we have shown that a single septin can efficiently polymerize in vitro. Thus, filament assembly in vitro does not require septin heteromultimers. Whether a single septin subunit can polymerize in vivo remains to be determined. It is conceivable that the general properties of septin polymerization that we have described by examining a single subunit may be generally applicable to the biochemistry of septin heteromultimers, though future experiments are necessary to establish this point.

The relationship between septin polymerization and septin function has been addressed previously. Cells carrying a deletion of the *CDC10* septin gene maintain many septin-dependent functions (localization of Bni4p, Bud4p, and the other septins to the bud neck, efficient cytokinesis) but lack neck filaments. Although the relationship between neck filaments and septin filaments is not entirely clear, this result indicates that highly ordered arrays of septin filaments are not required for septin function [3]. In vitro experiments showed that septin complexes purified from wild-type yeast cells associate into long, paired filaments upon dialysis into low-salt buffer. On the other hand, complexes purified from cells lacking the septin Cdc10p failed to assemble into filaments under the same conditions [3]. These data may indicate that septin function may not require septin filament assembly [1, 3]. Alternatively, septin complexes lacking Cdc10p could assemble into filaments that do not form highly ordered arrays in vivo and are incompetent to assemble under the conditions used in these in vitro experiments. The evolutionary conservation of the motifs required for GTPase activity strongly suggests that this activity is required for septin function. In this report, we have presented evidence that GTP binding, though not GTP hydrolysis, is intimately linked to septin polymerization. It is therefore likely that GTP-dependent filament assembly is critical for septin function in vivo.

Although the results presented here shed light on some aspects of septin filament assembly, many key issues remain to be addressed. Most importantly, it is still unclear how the filamentous state of septins correlates with their biological function. The ability to generate septin mutants, characterize their ability to assemble into filaments in vitro, and then monitor the phenotype of such mutations in vivo should help elucidate this problem.

Experimental Procedures

Purification of *Xl Sept2*

The coding sequence of *Xl Sept2* (GenBank accession number AF212298) and the coding sequence minus the predicted coiled-coil domain (amino acids 309–356; identified according to [15]) were cloned in the pTYB4 vector (NEB) as an N-terminal in-frame fusion with the intein-CBD (chitin binding domain) coding sequence. Extracts of BL21(DE3) cells expressing the *Xl Sept2*-intein constructs were loaded into a chitin-agarose column, and affinity purification was performed according to the manufacturer's instructions. After DTT-induced cleavage of the intein-CBD moiety, the protein was eluted from the column, dialyzed against buffer S (20 mM Tris [pH 8.0], 20 mM NaCl, 20% glycerol, 1 mM MgCl₂, 0.1% Triton X-100), and stored at –80°C at a concentration of 1–2 mg/ml.

GTP Binding and Hydrolysis Assays

For GTP binding, 1 μ M *Xl Sept2* (or Δ cc-Sep2) in S buffer was incubated with 0.1 mg/ml BSA, 5 mM MgCl₂, and 4.4 μ M [³H]GTP

(4.60 Ci/mmol, 1 mCi/ml; Amersham). At time intervals, aliquots of the reaction were diluted in ice-cold wash buffer (20 mM Tris [pH 8.0], 50 mM NaCl, 5 mM MgCl₂) and filtered through prewetted nitrocellulose (NC) circles (Schleicher and Schuell). Filters were washed with 10 ml wash buffer and dried, and the retained radioactivity was quantified in a scintillation counter. For the competition experiment, 1 μ M *Xl* Sept2 was incubated with 4.4 μ M [³H]GTP and various concentrations of unlabeled GTP, GDP, GTP- γ -S, and ATP for 60 min at room temperature before filtering as described above. For GTP hydrolysis, 1 μ M *Xl* Sept2 was incubated with [α -³²P]GTP (800 Ci/mmol, 10 mCi/ml) or GTP- γ -[³⁵S] (1133 Ci/mmol, 1 mCi/ml, Amersham) as described above. At time intervals, aliquots were diluted in denaturing solution (1% SDS, 20 mM EDTA), heated at 65°C for 10 min, and spotted on a PEI-cellulose plate (Macherey-Nagel). TLC plates were developed in 1 M LiCl, air-dried, and GTP, GDP, and Pi spots were quantified by phosphorimaging. The fraction of hydrolyzed nucleotide was calculated as GDP/(GTP + GDP) or Pi/(GDP + Pi). Nucleotide R_f values were confirmed by visualizing unlabeled standards with UV light. The mobility of the thio-phosphate group released from GTP- γ -[³⁵S] was confirmed by treatment with alkaline phosphatase (Boehringer) and phosphorimaging.

In order to identify the nucleotide bound to *Xl* Sept2, [α -³²P]GTP was included in the binding assays, the NC filters were treated with denaturing solution, and the released nucleotide was analyzed by TLC as described above.

Analysis of Nucleotide Associated with Polymeric Septin

Precleared *Xl* Sept2 (25 μ M) was incubated with [α -³²P]GTP (500 μ M) for 60 min. Assembly reactions (25 μ l) were centrifuged through 100 μ l of a 60% glycerol cushion (279,000 \times g, 20 min at 4°C). The supernatant and cushion were aspirated, and the pellet was resuspended in 1% SDS/20 mM EDTA. Totals and pellet fractions were analyzed by SDS-PAGE, followed by Coomassie staining and by TLC described as above.

Filament Immunofluorescence and Negative Staining

Polymerization reactions were carried out in buffer S in the presence of 5 mM MgCl₂ and the indicated nucleotide. Before nucleotide addition, all samples were prespun in an ultracentrifuge (279,000 \times g, 20 min at 4°C). For immunofluorescence, aliquots of the reaction (25 μ M septin, 100 μ M nucleotide) were diluted in buffer S to a final septin concentration of 3.3 μ g/ml, and 100 μ l drops were spotted on aminopropylsilane-treated coverslips. One minute after sample application, the coverslips were washed with 2 ml buffer S, fixed in -20°C methanol, and stained with a polyclonal rabbit antibody raised against a peptide comprising the 16 amino-terminal residues of *Xl* Sept2 (M.G. and A.A.H., unpublished data). Images were acquired by using a Spot II cooled CCD camera (Diagnostic Instruments) mounted on a Zeiss Axioplan II microscope and were processed with MetaMorph software (Universal Imaging) or Adobe PhotoShop. For electron microscopy, samples (25 μ M septin, 500 μ M nucleotide) were applied to carbon-coated grids for 5 min. The grids were rinsed with a drop of S buffer, stained with two drops of 1% uranyl acetate, and viewed in a CM120 BioTwin electron microscope (Philips).

Light Scattering

Xl Sept2 in S buffer was centrifuged as above and was placed in a quartz cuvette in a LS50B spectrometer (Perkin Elmer). The sample was illuminated with 350-nm light, and the scattered light at the same wavelength was collected at a 90° angle. After a stable baseline was obtained, the cuvette was removed from its position in order to add 0.5 mM nucleotide and MgCl₂ to 5 mM, and its contents were rapidly mixed before repositioning the cuvette. The temperature in the cuvette was maintained at 20°C throughout all of the experiments by using a water cooling system. For estimation of the critical concentration, steady-state assembly reactions were subjected to serial dilutions in S buffer containing 0.5 mM nucleotide and were placed in a water bath at 20°C for 2 hr. Scatter measurements of each dilution were performed for 20 or more min to ensure that a stable polymerization level had been reached. All intensity measurements are given in arbitrary units; the light scattered by buffer alone was subtracted from the plotted values. Data points

were collected every second and were analyzed with WinLab (Perkin Elmer).

Acknowledgments

We are grateful to Karen Oegema, Roland Foisner, Christine Field, Tim Mitchison, and members of the Glotzer and Knoblich labs for helpful discussions. We thank Ken Goldie for assistance with electron microscopy. We thank Jürgen Knoblich, Jan Michael Peters, and Kim Nasmyth for critical review of the manuscript.

Received: June 5, 2002

Revised: August 19, 2002

Accepted: August 29, 2002

Published: October 29, 2002

References

1. Field, C.M., and Kellogg, D. (1999). Septins: cytoskeletal polymers or signalling GTPases? *Trends Cell Biol.* 9, 387–394.
2. Field, C.M., al-Awar, O., Rosenblatt, J., Wong, M.L., Alberts, B., and Mitchison, T.J. (1996). A purified *Drosophila* septin complex forms filaments and exhibits GTPase activity. *J. Cell Biol.* 133, 605–616.
3. Frazier, J.A., Wong, M.L., Longtime, M.S., Pringle, J.R., Mann, M., Mitchison, T.J., and Field, C. (1998). Polymerization of purified yeast septins: evidence that organized filament arrays may not be required for septin function. *J. Cell Biol.* 143, 737–749.
4. Hsu, S.C., Hazuka, C.D., Roth, R., Foletti, D.L., Heuser, J., and Scheller, R.H. (1998). Subunit composition, protein interactions, and structures of the mammalian brain sec6/8 complex and septin filaments. *Neuron* 20, 1111–1122.
5. Kinoshita, M., Kumar, S., Mizoguchi, A., Ide, C., Kinoshita, A., Haraguchi, T., Hiraoka, Y., and Noda, M. (1997). Nedd5, a mammalian septin, is a novel cytoskeletal component interacting with actin-based structures. *Genes Dev.* 11, 1535–1547.
6. Beites, C.L., Xie, H., Bowser, R., and Trimble, W.S. (1999). The septin CDCrel-1 binds syntaxin and inhibits exocytosis. *Nat. Neurosci.* 2, 434–439.
7. Adam, J.C., Pringle, J.R., and Peifer, M. (2000). Evidence for functional differentiation among *Drosophila* septins in cytokinesis and cellularization. *Mol. Biol. Cell* 11, 3123–3135.
8. Bourne, H.R., Sanders, D.A., and McCormick, F. (1991). The GTPase superfamily: conserved structure and molecular mechanism. *Nature* 349, 117–127.
9. Macara, I., Baldarelli, R., Field, C.M., Glotzer, M., Hayashi, Y., Hsu, S.-C., Kennedy, M.B., Kinoshita, M., Longtime, M., Low, C., et al. (2002). Mammalian septin nomenclature *Mol. Biol. Cell*, in press.
10. Cooper, J.A., and Pollard, T.D. (1982). Methods to measure actin polymerization. *Methods Enzymol.* 85, 182–210.
11. Kang, F., Purich, D.L., and Southwick, F.S. (1999). Profilin promotes barbed-end actin filament assembly without lowering the critical concentration. *J. Biol. Chem.* 274, 36963–36972.
12. Romberg, L., Simon, M., and Erickson, H.P. (2001). Polymerization of Ftsz, a bacterial homolog of tubulin. Is assembly cooperative? *J. Biol. Chem.* 276, 11743–11753.
13. Pfannstiel, J., Cyrklaff, M., Habermann, A., Stoeva, S., Griffiths, G., Shoeman, R., and Faulstich, H. (2001). Human cofilin forms oligomers exhibiting actin bundling activity. *J. Biol. Chem.* 276, 49476–49484.
14. Oosawa, F., and Kasai, M. (1962). A theory of linear and helical aggregations of macromolecules. *J. Mol. Biol.* 4, 10–21.
15. Lupas, A., Van Dyke, M., and Stock, J. (1991). Predicting coiled coils from protein sequences. *Science* 252, 1162–1164.